RISING WATER TABLE AND SEISMICITY

N.D. Fowkes*, G. Hocking†, C.P. Please‡, D.P. Mason§ and R. Kgatle¶

Other Study Group participants:
Aminat Oyiza Suleiman, Charles Fodya, Salome Mogole,
Zinhle Sangweni, Derwin Ngomane and Maudu Hamese

Industry representatives
Nielen van der Merwe and Halil Yilmaz

Abstract

The old closed mines in the Witwatersrand are flooding and there is concern that the water may seep into stable faults in the neighbourhood and thus destabilise them. The simple models described here suggest that the time span for water transport into such faults is likely to be relatively short (months) and that, for deep mines (2000m-3000m) the hydrostatic pressure buildup within the filled cracks is likely to significantly increase the risk of fault slip. The effective coefficient of friction is predicted to reduce by $20-30\%$ due to fault flooding in such circumstances. Furthermore slip is predicted to occur along faults not previously prone to slip because of their 'unfavoured' orientation. Seismic

*Mathematics Department, University of Western Australia, Crawley, WA 6009, Australia *email: neville.fowkes@uwa.edu.au*

†Mathematics and Statistics, FSE Murdoch University, Murdoch, WA 6150, Australia *g.hocking@murdoch.edu.au*

‡School of Mathematics, University of Southampton, Southampton SO17 1BJ UK. *email: colinplease@gmail.com*

§School of Computational and Applied Mathematics, University of the Witwatersrand, Private Bag 3, WITS 2050, Johannesburg, South Africa. *email: David.Mason@wits.ac.za*

¶School of Computational and Applied Mathematics, University of the Witwatersrand, Private Bag 3, WITS 2050, Johannesburg, South Africa. *email: mrr.kgatle@gmail.com*

events are also more likely to cause slip because of lubrication effects. Under such circumstances, and in the absence of remedial action (say through improved sealing of the tunnels or pumping), Johannesburg could experience an increase in small seismic events.

1 Introduction

Gold mines consist of a network of vertical shafts with various connected tunnels, drives and crosscuts introduced to access the gold reef and remove products. The removal of rock effects the loading on faults and thus leads to increased seismic activity (hundreds of small seismic events per year are experienced as a direct result), see Gibowicz and Lasocki (2000), and Fowkes, Mason and Napier (2004). Of more direct concern here is the increased cracking in the general mining area and especially the localised fracturing adjacent to the excavations (within a distance of 1 or 2 meters) which can help facilitate water transport into adjacent faults.

Before mining is undertaken water deposited on the land through rainfall is carried to the oceans either over the land or in aquifers that in context are typically 300m in depth (but can be 1000m or greater in sedimentary zones). Below this zone the rock is dry. In mined areas water can accumulate in the shafts and is pumped out to facilitate the operations, but once the mining activity has ceased the water accumulates within the shafts and the fractured surrounds, see Figure 1. The depth of water in such abandoned tunnels (2 to 5m wide and 3.5m high) can typically increase at about 1 to 2 metres per day under wet conditions. The concern is that the water may then enter into faults that are hydrologically connected to the mining network thus lubricating them[1]. The nature of the hydraulic connection would not be normally known and may vary in time. The faults themselves can vary in width from fractions of millimetres up to a few millimetres or greater and often have offsets (perhaps 10 metres spacing) so there is much uncertainty about the hydraulic conductivity along these faults. Also there may be faults that intersect the wet surface layer; these faults would normally be water logged. Can the presence of this water in abandoned shafts lead to an increased incidence of seismic events subsequently? Evidently the problem separates out into two subproblems: the water transport problem treated in Section 2, and the fault-slip problem treated in Section 3. In Section 4 there is a brief discussion of the effect of

[1] assuming the rock is wettable

water on the behaviour of faults under external seismic loading. Conclusions are drawn in Section 5.

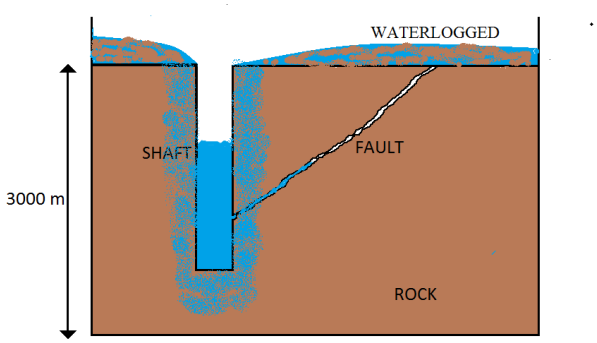

Figure 1: Water movement through mines and into faults

2 Water Flow in Faults

As indicated above there is a great deal of uncertainty about the hydrological conductivity of the fault so that the models developed here are necessarily speculative and would need to be calibrated to take into account local fault and field conditions. What is reasonably well known on site is the hydraulic head driving the flow[2]. The fault angle can also be readily determined using seismic measurements. The (geometry of) the hydraulic linkage between the tunnel network and the fault will vary depending on circumstances and this will strongly affect water transport. We will examine a few possible situations and then make general comments. Two simple models were developed, a thick fault model and a thin fault model.

2.1 A thick fault

For thick faults (thickness greater than 0.5cm say) the hydraulic conductivity is determined primarily by the permeability of the crushed material (created by seismic activity) filling the fault. In this case we can model water flow in

[2]It would appear that the water level in the various tunnels/shafts etc is the same which one would expect given the size of the excavations.

the crack as a porous medium flow between impermeable rock faces, see Figure 2. For simplicity we assume the shaft continues to fill from above in such a way that the height of water in the shaft remains fixed.

The flow of a liquid through a porous medium can be studied by defining the piezometric head

$$\Phi = \frac{p}{\rho_w g} + z, \tag{1}$$

where z is elevation above a datum here taken as the bottom of the shaft as in Figure 2; p is the pressure, ρ_w is water density and g is gravitational acceleration. The usual model assumes the flow is dictated by Darcy's Law, see Harr (1962), Bear (1972), which states that the D'Arcy velocity (average volume flux) $\mathbf{u}$ is given by

$$\mathbf{u} = -\kappa \nabla \Phi, \tag{2}$$

where the hydraulic conductivity $\kappa = \rho_w g k/\mu$, where k is the coefficient of permeability of the material and μ is the dynamic viscosity of the fluid. The pressure at the bottom of the shaft is $\rho_w g H_w$, so the total potential of a particle at the bottom of the shaft is given by $\Phi(0) = H_w$. If $z = h(t)$ is the height of the column of water in the fault above the shaft base, see Figure 2, then the total potential of a particle on the surface of this column is $\Phi(h) = h(t)$, so the driving potential in the fault is $(H_w - h(t))$ and the vertical flux $w = \kappa(H_w - h(t))/h(t)$, see (2). Now $w = h'(t)$ so that

$$\frac{dh}{dt} = \frac{\kappa(H_w - h)}{h}, \tag{3}$$

and if we assume the crack is initially dry then $h(0) = 0$. The solution can be written in the form

$$t = -\frac{1}{\kappa}\left[h + H_w \ln\left(\frac{H_w - h}{H_w}\right)\right], \tag{4}$$

giving the time t for the water to reach height h. We can estimate the time for the crack to fill to 90% of the water depth in the shaft by letting $h = 0.9H_w$, giving

$$t_{90} = -\frac{H_w}{\kappa}\left[0.9 + \ln(0.1)\right] \approx 1.5\frac{H_w}{\kappa} \tag{5}$$

The coefficient of permeability takes typical values of $\kappa \approx 1$ cm/s for gravel and $\kappa \approx 10^{-3}$ cm/s for fine sand, see Harr (1962). Assuming the crack is filled with crushed matter approximating fine sand this gives an estimate time

of $t_{90} \approx H_w/\kappa \approx 10^4/10^{-3} \approx 10^7$ sec. for $H_w \approx 300$m, that is, around 500 days. The fastest fill time would be of the order of days if the crack contained material with gravel-like properties, but this seems unlikely given the pressures at these depths.

These results suggest that in a relatively fast time significant portions of the fracture could be filled with water, but that the variation could be huge depending on the properties of the debris in the crack. Even if the filling takes a year, however, if there is no remedial action it will eventually fill and lubrication of the fractures will become an issue. Some pumping out of the original shaft may delay this problem.

2.2 A thin fault

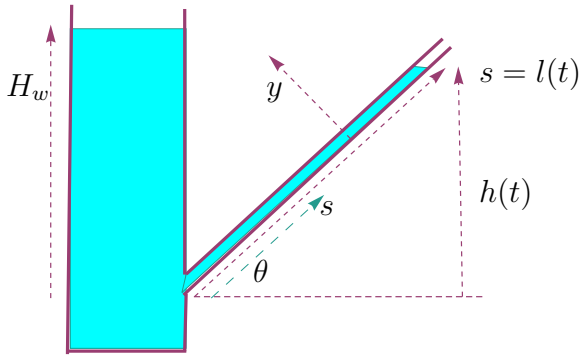

Figure 2: Water flow up a fault of width w from a shaft.

If the fault is thin then we have channel flow between two walls separated by a distance of w say, fed by water in the mining shaft. The simplest possible (2D) geometry is as shown in Figure 2; we have flow up a fixed width planar fault at an angle θ to horizontal intersecting a vertical shaft containing water. As before we will assume that the water level in the shaft measured from the intersection with the fault remains fixed at H_w, and that initially the height of water in the fault is given by $h(0) = 0$, where $h(t)$ height in the fault at time t measured from the junction. Evidently the water level in the fault will eventually reach H_w and our aim is to determine the characteristic time required for this to happen.

The flow up the fault is quasi-steady and viscosity dominated and the geometry is thin, so that the Navier-Stokes equations reduce to a single equation describing flow along the fault given by

$$\frac{\partial p}{\partial s} = \mu \frac{d^2 u}{dy^2} - \rho_w g \sin\theta \quad \text{with } p = p(s,t), \quad \text{and } \mathbf{v} = u(y,t)\hat{\mathbf{s}}, \tag{6}$$

where s is the distance along the fault measured from the junction, $\hat{\mathbf{s}}$ is a unit vector in the direction of the flow along the fault, and y measures distance from the lower fault face as in Figure 2.

Choosing atmospheric pressure as the datum the appropriate boundary conditions are given by

$$p = \rho_w g H_w \text{ at } s = 0, \text{ with } p = 0 \text{ at } s = l(t) = h(t)/\sin\theta,$$

see Figure 2. Subject to these conditions and using separation of variables the solution to (6) is given by

$$p(s,t) = \rho_w g H_w \left[1 - \frac{s}{l(t)}\right], \quad \text{with} \quad u = -\frac{1}{2\mu}\left[\rho_w g \sin\theta + \frac{\partial p}{\partial s}\right] y(w-y), \tag{7}$$

or equivalently

$$u = \frac{\rho_w g}{2\mu}\left[\frac{H_w - h(t)}{l(t)}\right] y(w-y), \tag{8}$$

using (7). The net volume flux up the fault (per unit fault depth) is thus given by

$$\int_0^w u(y,t)dy = \frac{\rho_w g w^3}{12\mu}\left[\frac{H_w - h(t)}{l(t)}\right].$$

For later purposes note that it is the 'modified' pressure difference $\rho_w g(H_w - h(t))$ acting over the length $l(t)$ that drives the channel flow[3]
The average velocity determines the front speed giving

$$< u >= \frac{1}{w}\int_0^w u(y,t)dy = \frac{dl}{dt} = \frac{\rho_w g w^2}{12\mu}\left[\frac{H_w - h(t)}{l(t)}\right],$$

[3]The flux through a horizontal channel of width w due to an applied pressure gradient p_x is $\rho_w g p_x w^3/(12\mu)$.

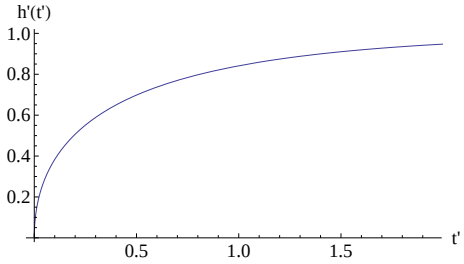

Figure 3: The (scaled) hydraulically driven water movement $h'(t')$ from a shaft into a fault.

so that eliminating $l(t)$ in favour of $h(t)$ gives

$$\frac{dh(t)}{dt} = \left[\frac{\rho_w g w^2 \sin^2\theta}{12\mu}\right](\frac{H_w - h(t)}{h(t)});$$

an ordinary differential equation for the moving front. Scaling the equation thus:

$$h(t) = H_w h'(t'), \quad \text{with} \quad t = Tt', \quad \text{where} \quad T = \frac{12\mu H_w}{\rho_w g w^2 \sin^2\theta}, \tag{9}$$

we obtain the equation

$$\frac{dh'}{dt'} = \frac{1 - h'(t')}{h'(t')},$$

with the implicit solution given by

$$t' = -\ln|1 - h'(t')| - h'(t')$$

after applying the initial condition $h'(0) = 0$; this corresponds to (4) obtained for the thick fault. During the initial filling stages the fault fills rapidly (like $\sqrt{2t'}$) and the level approaches that of the water within the shaft like $1 - h' = \exp(-t')$, see Figure 3. Effective equilibrium is thus reached when $1 - h' \approx 0.06$ that is when $t' \approx 5$ which gives a characteristic fault filling time of

$$t_f = \frac{60\mu H_w}{\rho_w g w^2 \sin^2\theta}.$$

The filling time increases very rapidly with decreasing fault thickness (like $1/w^2$) and varies in proportion to $1/\sin\theta$, because of the increased length of the water column in the faults. With $\mu = 8.910^{-4}$Pa.sec, $\rho_w = 10^3$kg/m^3, $g = 9.8$m/sec^2, and $w = 0.1$mm we obtain 17 days to 50 days as the fault angle decreases from 60° to 30°. For $w = 1$mm we obtain hours rather than days.

2.3 Leakage models

The above simple models provide a time scale ranging from hours to weeks for equilibrium to be reached under 'ideal model' conditions. The results for the characteristic times for the thin and thick fault models are comparable basically because it is the size of the gaps between the solid surfaces that determines the seepage time; recall the thick fault is filled with crushed material. The time scales vary somewhat depending on the fault structure but in the mining context all of the above time scales are short. Thus, within a year after water pumping ceases one can expect water to seep into and 'fill' neighbouring faults. The models are of course very simple and assume there are no 'major' blockages to flow. Note however that under significant hydraulic head (as in our case) water will 'seek out' conducting paths of 'least resistance', so that flow rates of the same order as above would be expected with smaller flow rates through many low conductivity paths over a compensating larger region; primarily it is the head that determines the flow. The statement stands; the time scale is expected to be 'relatively short'.

There is however a major limitation to the applicability of the above models. In both the above models the hydraulic systems are hydraulically closed so that eventually such systems will equilibrate with water levels in all portions of the hydraulic network matching. In practice there is likely to be leakage from the system which means that the extent of seepage will be determined by a balance between water flow into the system and leakage from the system. Thus, whilst the above results do provide useful seepage time scale estimates, they cannot really provide a practical estimate for the extent of water incursion into the fault zone. What really is required is a practical way of assessing this in terms of measurable quantities. Probably the only available measurable information is water depth as a function of time in shafts in the mining area. As shown in the above models there is a significant slow down in the seepage rate into faults close to equilibrium which would be accompanied by a corresponding slow down in the water level changes in the feeding shafts. It may be that simple leakage models can be usefully used to obtain quantitive information. It will be recalled that the effective driving pressure is the modified pressure. Using this it should be possible to estimate the extent of seepage in various directions.

3 Fault slip

3.1 Slip in the absence of water

In regions excluding tunnels and faults the equations of static equilibrium and the compatibility equation for the Earth's stresses are given by

$$\tau_{xx,x} + \tau_{xy,y} = 0, \tag{10}$$

$$\tau_{yy,y} + \tau_{xy,x} = -\rho_r g, \tag{11}$$

$$\bigtriangledown^2(\tau_{xx} + \tau_{yy}) = 0, \tag{12}$$

where the x axis is horizontal, the y axis vertically upwards measured from the Earth's surface; ρ_r is the rock density. Assuming an initial relaxed stress state (that is, with no unresolved shear) we have

$$\tau_{xx,x} = 0,\ \tau_{yy} = -\rho_r g y,\ \tau_{xy} = 0.$$

The driving force in the vertical direction is of course gravity, so the vertical normal stress is hydrostatic. Note however the horizontal variation in stress τ_{xx} is undetermined under equilibrium conditions until one specifies boundary conditions at $x \to \pm\infty$; one must specify how the geological structure is supported. Of course the support mechanism is very dependent on the formation and subsequent history of the geological structure, and sedimentary rock formations and volcanic rock formations are likely to be supported in very different ways. There is also considerable uncertainty as far as any formation is concerned, and very little available structural data to work with. Furthermore there are normally cracks throughout the structure so that the effective elastic properties are not those of a simple solid and will change with time. Any geological structure will in fact continuously creep. Heim has suggested that under such conditions the stress distribution will tend towards hydrostatic, a situation referred to as *lithostatic*. Under such hydrostatic circumstances $\tau_{xx} = \tau_{yy} = -\rho_r g y$. This result is referred to as Heim's rule; the system behaves like a fluid contained in a solid containment vessel. If, on the other hand, the structure is unconstrained horizontally so that it is entirely self supporting then $\tau_{xx} = 0$. The region of interest may be either compressed or stretched by its containing vessel and the rock is normally fractured in most geological conditions, so that it is weak under tension. Thus only compression seems

sustainable[4]. In order to model a range of practical circumstances we will use a 'k' model given by

$$\tau_{xx} = -k\rho_r g y, \text{ with } 0 \leq k \leq 2; \tag{13}$$

one would expect stresses to scale up 'hydrostatically'. One would expect $k \approx 1$ for sedimentary formations with k smaller or larger under external loading.

Mining will of course affect the stress distribution locally and more importantly will affect the loading on faults. In regions close to excavations the fault will be unloaded, and so more likely to slip. Such considerations are important in the present context and such issues have been addressed in a previous MISG in a different context, see Fowkes, Mason and Napier (2004), however here we will only consider the simpler k models.

3.2 Fault slip under k loading

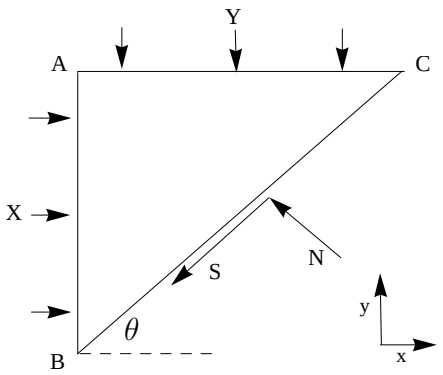

Figure 4: Stresses acting on a wedge of rock ABC in contact with a fault plane BC at angle θ to the horizontal.

If (X, Y) are the stresses acting on the vertical and horizontal faces of wedge of rock ABC in contact with a fault/slip plane at angle θ to the horizontal, and (N, S) are the normal and shear stresses acting on the wedge across the

[4]Under tension the material would crack thus releasing the tension.

fault face as in Figure 4, then (with the adopted sign convention) horizontal and vertical static equilibrium conditions for the wedge require

$$N\sin\theta + S\cos\theta = X\sin\theta,$$

$$N\cos\theta - S\sin\theta = Y\cos\theta,$$

in the limit as the wedge size goes to zero. Solving for (N, S) we obtain

$$N = X\sin^2\theta + Y\cos^2\theta, \quad S = (X-Y)\sin\theta\cos\theta.$$

Now $X \equiv -\tau_{xx}$ and $Y \equiv -\tau_{yy}$, with $X = k\rho_r gH$, $Y = \rho_r gH$ for the 'k' model, so the normal and shear forces acting across the fault face are given by

$$N/(\rho_r gH) = k\sin^2\theta + \cos^2\theta, \quad S/(\rho_r gH) = (k-1)\sin\theta\cos\theta, \tag{14}$$

plotted in Figure 5 for $0 < k < 2$ over the wedge angle range $0 \le \theta \le \pi/2$. The wedge will slip if $|S| > \mu_0 N$ where μ_0 is the frictional coefficient, that is, if $\mu_0 < \mu_{\rm crit}$ where the 'slip function'

$$\mu_{\rm crit}(k,\theta)) = \frac{|(1-k)|\sin\theta\cos\theta}{\cos^2\theta + k\sin^2\theta}, \tag{15}$$

defines the critical slip condition. Note, see Figure 5:

- $S > 0$ if $k > 1$, and (under such vessel compression circumstances) the wedge will slip up the fault plane for sufficiently small μ_0.
- $S < 0$ if $k < 1$, and the wedge will slip (gravitationally fall) down the fault plane for sufficiently small μ_0.
- Under lithostatic conditions $k = 1$ so $S = 0$; the wedge will not slip irrespective of wedge angle and μ_0. Under such circumstances the force transmitted across the fault is always normal to the fault face.
- The normal stress N acting on the wedge increases as the wedge angle θ increases in the $k > 1$ (that is, higher than lithostatic compression) case, and decreases in the case in which the region is under less than lithostatic compression. In the lithostatic ($k = 1$) case N remains fixed as the wedge angle varies.

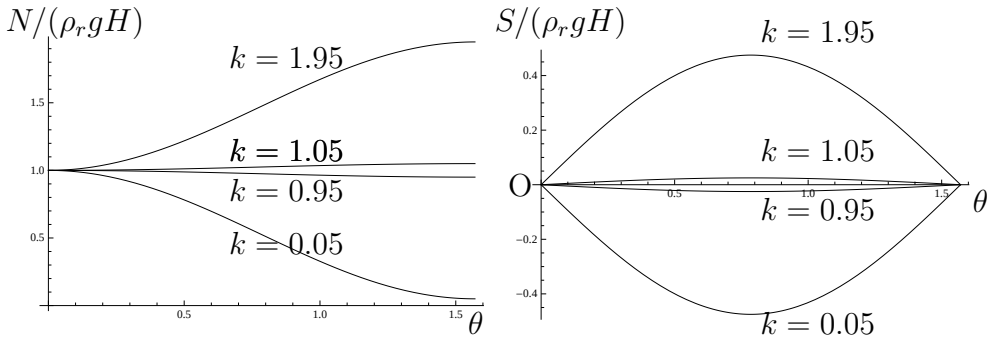

Figure 5: The normal and shear forces acting on a fault at angle $0 < \theta < \pi/2$, for $k = 0.05, 0.95, 1.05, 1.95$: *Left:* $N(k,\theta)/(\rho_r g H)$. *Right:* $S(k,\theta)/(\rho_r g H)$.

By plotting the slip function $\mu_{\text{crit}}(\theta)$ one can identify the fault angle range $(\theta_{\min}(\mu_0) < \theta < \theta_{\max}(\mu_0))$ corresponding to a prescribed μ_0. In Figure 6 the slip function is plotted out as a function of wedge angle for a small k case and a large k case. For decreasing μ_0 in the $k \gg 1$ (large compression) case slip first occurs (up the plane) for small fault angles, whereas in the $k \ll 1$ (gravity driven) case slip first occurs (down the plane) for large fault angles. In almost lithostatic ($k \approx 1$) cases faults at an angle of $\pi/4$ first slip.

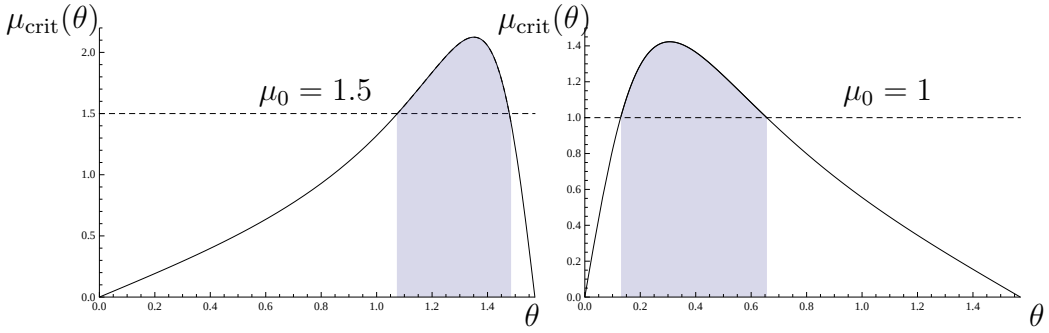

Figure 6: The slip function: *Left:* A small k case ($k = 0.05$). The slip fault angle range corresponding to $\mu_0 = 1.5$ is shaded. *Right:* A large k case ($k = 10$). The slip fault angle range corresponding to $\mu_0 = 1$ is shaded.

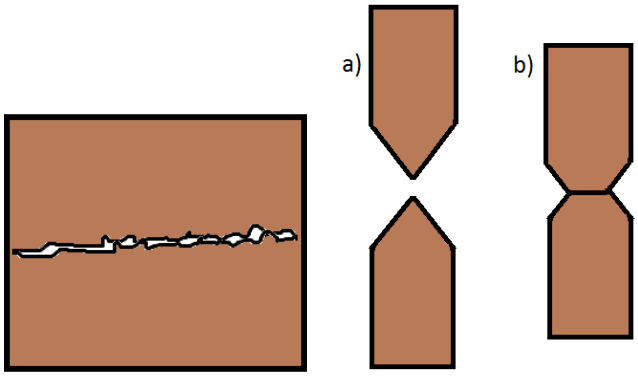

Figure 7: Contact between rock surfaces: asperities.

3.3 Friction models: the dry rock case

Rough surfaces (including rock faces) make contact only at high points called asperities (see Figure 7), so that the real contact area between the surfaces is very much less than the apparent area under normal (engineering) conditions (ratios of the order of 10^{-3} are typical), and the associated real stresses (real force/real area) are correspondingly very large. The asperities in contact compress/crush each other to the extent required to support the load and it is classically assumed that the real normal stress remains fixed with increased loading and is given by the yield stress σ_{crit}[5]. Thus the normal stress N acting on the fault plane and the fractional contact area between the two faces A_{real} are related thus

$$N = A_{\text{real}}\sigma_{\text{crit}}; \tag{16}$$

σ_{crit} can be determined experimentally and so A_{real} can be inferred for prescribed loading.

Also slip involves shearing of the asperities, so that slip conditions can be related back to the shear strength τ_{crit} of the material; we have

$$|S_{\max}| = A_{\text{real}}\tau_{\text{crit}}, \tag{17}$$

and, since in both cases the stresses act over A_{real} *under dry contact*, we have

$$\tau_{\text{crit}} = \mu\sigma_{\text{crit}}.$$

[5]Experimentally one finds that there is a slow increase in real normal stress with increasing loading until a plateau is reached, see Persson (2002)

The above 'laws' of frictional behaviour are referred to as Amonton's first and second laws. These laws were first established and verified in metal contact (engineering) contexts where contact areas are relatively small and elastic/elastoplastic forces dominate, but were found to work in much higher contact circumstances where adhesive forces play a role, see Persson (2006). They are also known to work in brittle rock situations, and so are generally assumed to work in fault slip contexts although geological pressure levels are much larger and the contact surfaces are polished by previous movements, see Scholz (1998).

Aside: Theoretical results have been obtained determining the real contact area as function of real normal stress in terms of the roughness power spectrum and elastic/adhesive properties of the material, see Persson (2006). Such results may be useful in the geological context. There appears to be no experimental verification for these results in the geological context. For more details see Greenwood and Williamson (1966), Greenwood and Tripp (1976), and for a recent review of contact theories see Persson (2006).

Aside: One might wonder if rocks behave like 'normal rocks' at the pressures of interest. The mine depths in South Africa are of the order of $2000 - 3000$m so hydrostatic (rock) pressure levels of the order of $40 - 90$MPa (using $\rho_r = 2$ to $3\ 10^3 \text{kg/m}^3, \text{g} = 9.8\text{m/sec}^2$) are expected[6]. The yield stress of rocks (silicates) are of the order of 500MPa, so one would not expect 'global plastic' behaviour of rocks at 3000m. The yield stresses are affected by temperature and pressure, both of which are large at the depths of interest however in context the effects are marginal, see Scholz (2002).

3.4 Slip after water entry

Water entering a fault will fill the 'free' (non real rock contact) spaces. Under equilibrium (water flow) conditions this water will be at hydrostatic pressure $\rho_w g H_w$, where H_w is the depth of water at the location of interest; at depths of the order of $2000 - 3000$m this will be significant (approx 30MPa; roughly half of the rock pressure). This water will take up part of the applied elastic stress N normal to the fault, thus reducing the area of real contact between the opposing faces from A_0 (under dry conditions) to A_w (under hydrostatic loading). Since the same normal force N needs to be supported as before, we

[6]The specific gravity of limestone is 2.3-2.7, basalt 2.8-3.0, quartzite 2.6-2.8.

have

$$N = A_w\sigma_{\rm crit} + (1 - A_w)\rho_w g H_w = A_0\sigma_{\rm crit},$$

see (16)), which determines the real area of contact under hydrostatic loading as

$$\frac{A_w}{A_0} = 1 - (\frac{1 - A_0}{A_0})(\frac{\Psi}{1 - \Psi}), \tag{18}$$

where

$$\Psi = \frac{\rho_w g H_w}{\sigma_{\rm crit}},$$

is the dimensionless group that determines the effect of water entry. Note that $A_w/A_0 \to 1$ (so there is little effect in the contact area) if either $A_0 \to 1$ (no water can enter) or $\Psi \to 0$ (small water depth).

Resistance to applied shear can only be provided by the contacting asperities (since water cannot provide resistance to shear under static loading), so that the maximum externally applied shearing force that can be resisted under hydrostatic loading will be reduced from $A_0\tau_{\rm crit}$ to $A_w\tau_{\rm crit}$, and thus the effective coefficient of friction under hydrostatic loading will be reduced in proportion to the contact area ratio: we have

$$\frac{\mu_w}{\mu_0} = \frac{A_w}{A_0} = 1 - (\frac{1 - A_0}{A_0})(\frac{\Psi}{1 - \Psi}). \tag{19}$$

Assuming (as above) that (1) the contact area pressure relationship is linear, (2) that the contact area is very small at the Earth's surface, and (3) that when the normal stress level reaches the yield level $\sigma_{\rm crit}$ there is complete contact between the opposing fault faces, we can estimate the real area of contact before entry as:

$$A_0 \approx \frac{\rho_r g D}{\sigma_{\rm crit}}, \tag{20}$$

where D is the depth at the location on the fault of interest. Using typical values for the parameters $\sigma_{crit} = 500 \times 10^6$Pa, $\rho_r = 3.10^3$kg/m^3 (corresponding to granite), and choosing a depth of 3000m we obtain $A_0 \approx 0.17$. Substituting this value into (19) gives

$$\frac{\mu_w}{\mu_0} \approx (1 - 0.30),$$

which represents a 30% change in μ/μ_0 at 3000m; *clearly significant!*

Note that the effective frictional coefficient decreases almost linearly with water depth H_w, see (18). Keeping the depth of fault location D fixed at 3000m

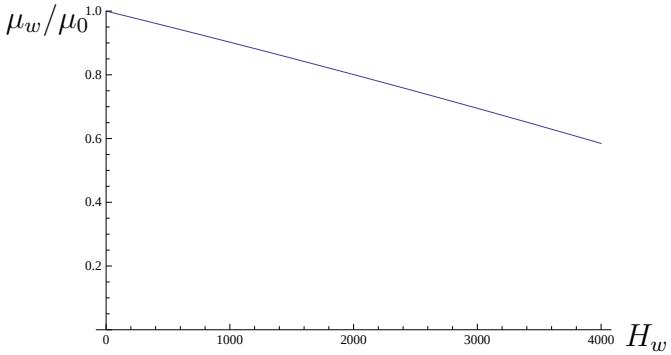

Figure 8: Proportional change in the coefficient of friction due to water entry. The water depth H_w is in metres.

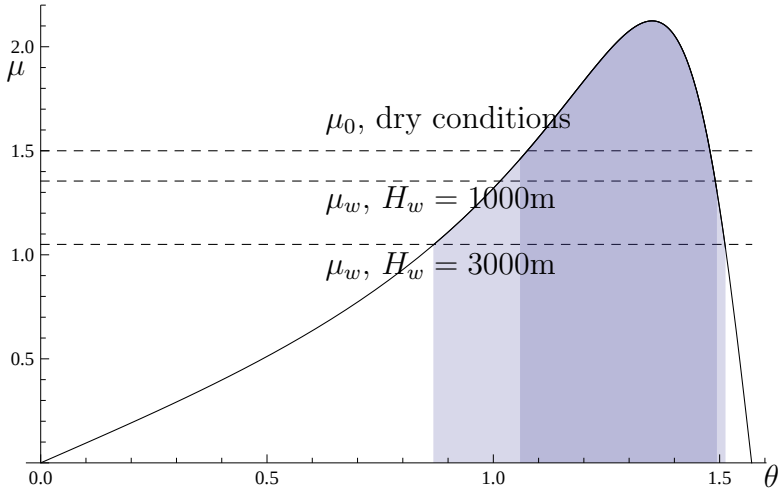

Figure 9: Water entry effects in the $k = 0.05$ case with $\mu = 1.5$ under dry conditions (upper dashed line) and corresponding μ_w values for water depths of $H_w = 1000$m (middle dashed line) and $H_w = 3000$m (lower line). Note especially that the range of fault angles for slip is increased significantly after water entry.

and varying the water depth H_w over the range $1000 - 4000$m we obtain the result shown in Figure 8.

Now of course whether the particular fault slips as a result of water inflow will depend on just how close it was to sliding in the first place, and we have seen that this depends on the orientation θ of the fault. For illustration in Figure 9 we examine the water entry effect in the $k = 0.05$ model displayed earlier in dry conditions, with water depths of 2000m and 3000m. Note especially that not only are fault planes within the dry failure θ range more prone to slip *but significantly also new α planes of weakness become slip prone.*

4 Seismic Events: Water effects

Seismic waves are long $>$ 1km for frequencies of seismic importance ($>$ 100 cycles/sec) so such waves are effectively vibrations over mining site distances. Thus the seismic situation can be modelled as an induced displacement of one face of the fault (the lower say) relative to the other face. The two faces are effectively 'elastically connected' via the asperities (modelled as springs) so the movement is partially resisted but shear stress levels will be enhanced, so fault slip can occur as a result of the event, depending on the stress status of the fault before the movement. The effect of water on this process can be dramatic because of lubrication effects in the thin water channels. In this context the incident angle of the oncoming seismic wave to the fault is of major importance because vibrations at right angles to the faults give rise to lubrication effects that can either promote fault separation (and thus slip) or resist separation (and thus prevent slip). This changed response is due to phase changes (essentially the phenomenon is a resonance situation). These issues have been examined in the context of the effect of mud on rock blasts, see Mureithi and Fowkes (2008). The effects can be dramatic as can be seen in the Figures 10 below, taken from this report. The circumstances were related so these results do raise further concerns. Further work will be necessary to examine such important (and subtle) issues in the present context.

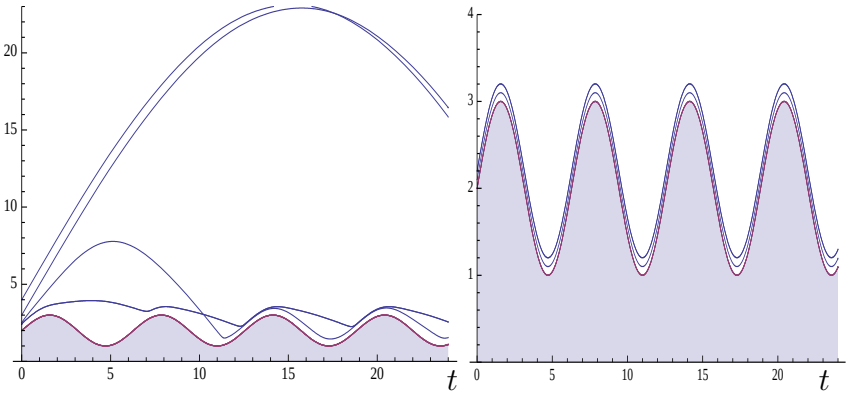

Figure 10: These figures display the effect of a vibration on the separation distance between rock faces when water fills the gap. The shaded region corresponds to one face of the rock and the other curves correspond to the movement of the second face under the action of a vibration. Depending on the separation of the faces and frequency of the vibration the faces may separate (left) or 'remain in contact' (right). In our present context slip would occur if the separation distance increases as in the left figure.

5 Conclusions

These investigations suggest that water will quickly seep into neighbouring faults and that, not only will slip prone faults be more likely to be triggered but also faults not active under dry conditions could now be active; an unexpected outcome. At 2000m our estimates suggest a 20% change in the effective frictional coefficient increasing to 30% at a depth of 3000m. The range of fault angles is greatly increased with angles both greater than and less than those previously 'active'. It should be emphasized that these results are based on a range of assumptions that need to be validated. Probably the most 'suspect' of the assumptions made is that the real area of contact between opposite faces of a fault increases in direct proportion to the applied normal load. This assumption is fine under engineering conditions but needs to be investigated under geological (high pressure, historic slip) conditions.

It also appears to be the case that external seismic events are more likely to trigger slip in water filled faults due to lubrication effects. Such effects are likely to be much more dramatic than expected in certain frequency ranges because of phase change effects. Given the complexity of our present situation

our state of understanding this must be regarded as speculative.

References

[1] Gibowicz, S.J. and Lasocki, S. (2000). Seismicity induced by mining: Ten years later. *Advances in Geophysics*, **44**, 39-167.

[2] Fowkes, N.D., Mason, D.P. and Napier, J.A.L. (2004). Fault slip in a mining context. *Proceedings of the Mathematics in Industry Study Group* 2004, Ed D. P. Mason pp 1-21.

[3] Bear, J. (1972). Dynamics of fluids in porous media. McGraw Hill.

[4] Harr, M. (1962). Groundwater and seepage. McGraw Hill.

[5] Greenwood, J. A., and Williamson, G. W. (1966). Multiasperity contact models. *Proc. R. Soc. London A* **295**, 300-319.

[6] Greenwood, J.A. and Tripp, J. (1976). The elastic contact of rough spheres. *J. Appl. Mech., Trans. ASME,* pp. 153-159.

[7] Persson, B.N.J. (2006). Contact mechanics for randomly rough surfaces. *Surface Science Reports* **61**, 201-227.

[8] Scholz, C. H. (2002). The mechanics of earthquakes and faulting. *Cambridge University Press 2nd Edn.*.

[9] Scholz, C.H. (1998). Earthquake and friction laws. *Nature* **391**, Jan, 37-42.

[10] Mureithi, E. and Fowkes, N. D. (2008). Rockburst and mud. *Proceedings of the Mathematics in Industry Study Group* 2008, Ed D. P. Mason pp 27-39.